Analysis of Cracked Laminates with Holes Using the Boundary Force Method

P. W. Tan* and C. A. Bigelow†
NASA Langley Research Center, Hampton, Virginia

In this paper, the Boundary Force Method (BFM), a form of an indirect boundary-element method, is used to analyze composite laminates with holes and cracks. The BFM uses the orthotropic elasticity solution for a concentrated horizontal and vertical force applied at a point in a cracked, infinite sheet as the fundamental solution. The necessary stress functions for this fundamental solution were formulated using the complex variable theory of orthotropic elasticity. The orthotropic formulation of the BFM was verified by comparison to accepted solutions for a center-crack specimen subjected to uniaxial tension. Four graphite/epoxy laminates were used: $[0/\pm 45/90]_s$, $[0]$, $[\pm 45]_s$, $[\pm 30]_s$. The BFM results agreed well with the accepted solutions. Parametric studies were done for two configurations for which no orthotropic solutions are currently available: cracks emanating from a circular hole and a four-hole cracked specimen, both loaded in uniaxial tension. In the specimen with cracks emanating from a hole, for small $2a/W$ ratios, when the hole dominated, the [0] laminate gave the highest stress-intensity correction factors, and the $[\pm 45]_s$ laminate gave the lowest values. For larger $2a/W$, when the effect of the hole had diminished, the trends were reversed, and the [0] laminate gave the lowest values of the stress-intensity correction factor; the $[\pm 45]_s$ laminate gave the highest values. For the four-hole specimen, the [0] laminate was the most sensitive to the presence of the holes, showing the greatest rise and drop in the stress-intensity correction factor as the crack approached and passed between the holes. The $[\pm 45]_s$ laminate showed the least effect due to the hole.

Nomenclature

a	= half-length of crack, m
A,B	= constants in stress functions, N/m^3
C_{ij}	= complex constants (i,j = 1,2)
E_x,E_y	= Young's moduli in the x- and y-directions, respectively, MPa
F	= stress-intensity correction factor
$[F]$	= influence coefficient matrix, N/m
G_{xy}	= orthotropic shear modulus, MPa
H	= height of plate, m
K_I	= mode I stress-intensity factor, MPa$\sqrt{\text{m}}$
N	= number of segments
$N(x),T(x)$	= normal and shear crack-face loading functions, MPa
p_i,q_i	= units loads on the ith segment, N
P,Q	= concentrated forces in the x- and y-directions, respectively, N
$\{P\}$	= vector of unknown forces, N
R_x,R_y	= x- and y-components of applied loading, N
$\{R\}$	= vector of external loads, N
S	= remote applied stress, MPa
t	= location of load point on crack face, m
w_i	= complex variable, (i = 1,4)
W	= width or half-width of plate, m
x,y	= Cartesian coordinates, m
z_0	= load point, ($z_0 = x_0 + iy_0$), m
δ_i	= incremental distance, (i = 1 to N), m
$\delta_1'(z),\phi_2'(z)$	= orthotropic stress functions, MPa
ν_{xy}, ν_{yx}	= Poisson's ratios
$\sigma_x, \sigma_y, \tau_{xy}$	= stresses, MPa
$\mu_1,\mu_2,\bar{\mu}_1,\bar{\mu}_2$	= roots of the characteristic equation

Received Feb. 17, 1987; presented as Paper 87-0862 at the AIAA/ASME/ASCE/AHS 28th Structures, Structural Dynamics, and Materials Conference, Monterey, CA, April 6-8, 1987; revision received Oct. 13, 1987.

*Research Engineer, Analytical Materials and Services.
†Research Engineer, Materials Division.

Introduction

In the field of fracture mechanics, stress-intensity factors are important parameters for predicting fracture strengths and fatigue lives. Analytical solutions for stress-intensity factors of cracked, finite bodies are not readily available and are often difficult to obtain. Thus, numerical techniques (e.g., the boundary-element method, the finite-element method, collocation) are widely used in computing stress-intensity factors. For isotropic materials, the necessary stress-intensity factors for finite-size sheets are often available from the literature. However, for orthotropic or composite materials, little is known about stress-intensity factors for finite-size laminates.

In this paper, the Boundary Force Method[1] (BFM), a form of an indirect boundary-element method, is used to analyze composite laminates that contain holes and cracks. For isotropic materials, the BFM has been shown to be an efficient, accurate method for determining the stress-intensity factors for complex crack configurations for which limited or no solutions are known.[1] In the current work, the BFM will be extended to orthotropic materials and used to analyze two complex crack configurations for which stress-intensity factor solutions are not currently available for orthotropic materials.

First, the BFM is briefly reviewed. For isotropic materials[1] the BFM uses the elasticity solution for concentrated horizontal and vertical forces and a moment applied at a point in a cracked infinite sheet as the fundamental solution. However, in the present formulation, the fundamental solution used is the orthotropic elasticity solution for a concentrated horizontal and vertical force applied at a point in a cracked, infinite sheet. The necessary stress functions for this fundamental solution are formulated using the complex-variable theory of orthotropic elasticity.[2] The orthotropic formulation of the BFM is evaluated by comparing the BFM results to accepted solutions for a center-crack specimen subjected to uniaxial tension. Para-

metric studies are done for cracks emanating from a circular hole and for a four-hole cracked specimen, both loaded in uniaxial tension; for these configurations, crack length-to-width ratios and material properties are varied to determine their effects on the stress-intensity factors. Four graphite/epoxy laminates are used: $[0/\pm 45/90]_s$, $[0]$, $[\pm 45]_s$, $[\pm 30]_s$.

Boundary Force Method

The BFM[1] is a numerical technique that uses the superposition of a finite number of sets of concentrated forces and moments in an infinite sheet to obtain the solution to the boundary-value problem of interest. For isotropic materials, the BFM uses the elasticity solution for a horizontal and a vertical concentrated force and a concentrated moment in an infinite cracked plate as the fundamental solution. The technique presented here uses only forces in the fundamental solution. The implications of this will be discussed later.

For orthotropic materials, the BFM uses the elasticity solution for a horizontal and a vertical concentrated force in a cracked, infinite sheet as the fundamental solution. (The derivation of the necessary stress functions for orthotropic materials is presented in the next section.) Since this fundamental solution models the crack faces and, thus, exactly satisfies the stress-free conditions there, the numerical analysis does not have to model the crack faces. Only the boundaries of the region of interest are modeled and, therefore, the only remaining conditions to be satisfied are the boundary conditions. The given boundary conditions are satisfied by applying sets of concentrated horizontal and vertical forces along an imaginary boundary, corresponding to the actual configuration, traced on an infinite sheet.

Consider, for example, the finite cracked plate subjected to uniaxial tension shown in Fig. 1. In the BFM, an imaginary boundary corresponding to the finite plate is traced on a cracked infinite sheet. These boundaries are then divided into a finite number of segments. On each segment, a concentrated force pair P_i and Q_i ($i = 1$ to N) are applied at a small distance δ_i on the outward normal from the midpoint of the segment. This small offset from the segment was used to eliminate the singularities in the computation of the stresses on the boundaries.

The concentrated forces P_i and Q_i acting on the ith segment produce stresses throughout the infinite plate. The stresses on each segment j are integrated over the segment length to find resultant forces on that segment. On each segment j, the sum of all the resultant forces in the x- and y-direction is equal to the externally applied force acting on the segment. The loading applied to the specimen boundaries is known and can be represented as horizontal and vertical applied forces R_{x_j} and R_{y_j} acting on each segment i. By equating the sum of the resultant forces due to P_i and Q_i ($i = 1$ to N) to the externally applied loads, we can write the following equations for the jth segment:

$$R_{x_j} = \sum_{i=1}^{N} (F_{x_j p_i} P_i + F_{x_j q_i} Q_i) \tag{1a}$$

$$R_{y_j} = \sum_{i=1}^{N} (F_{y_j p_i} P_i + F_{y_j q_i} Q_i) \tag{1b}$$

Here N is the total number of segments; $F_{x_j p_i}$, $F_{y_j p_i}$, $F_{x_j q_i}$, and $F_{y_j q_i}$ are called influence coefficients and are defined as follows:

$F_{x_j p_i}$ = force in the x-direction on the jth segment due to unit load p_i acting on the ith segment in the y-direction;

$F_{y_j p_i}$ = force in the y-direction on the jth segment due to unit load p_i acting on the ith segment in the y-direction;

$F_{x_j q_i}$ = force in the x-direction on the jth segment due to unit load q_i acting on the ith segment in the x-direction; and

$F_{y_j q_i}$ = force in the y-direction on the jth segment due to unit load q_i acting on the ith segment in the x-direction.

Thus, the resulting system of equations for N segments can be written as

$$[F]_{N\times N} \{P\}_{N\times 1} = \{R\}_{N\times 1} \tag{2}$$

where $[F]$ is the influence coefficient matrix, $\{P\}$ is the vector of unknown P and Q forces, and $\{R\}$ is the vector of externally applied forces. The influence coefficient matrix is square, fully populated, and nonsymmetric.

Because the influence coefficient matrix and the externally applied load vector are known, the unknown force vector can be obtained by solving the system of linear algebraic simultaneous equations. The calculated set of forces P_i and Q_i, acting on the imaginary boundaries in the sheet, will approximately satisfy the required boundary conditions and, thus, produce a stress distribution inside the imaginary boundaries that is approximately equal to the stress distribution of the desired boundary-value problem.

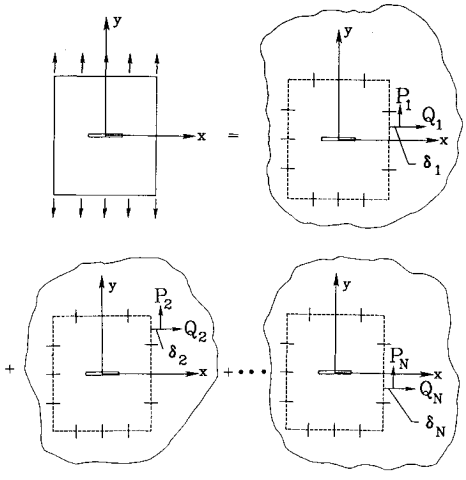

Fig. 1 Superposition of unknown forces P_i and Q_i on boundary segments, $i = 1$, N.

Derivation of Fundamental Solution for Orthotropic Materials

For orthotropic materials, the BFM uses the elasticity solution for a horizontal and vertical concentrated force in an infinite orthotropic sheet with a crack. The formulation of this solution is presented below.

Stresses in Orthotropic Materials

From Lekhnitskii[2] the stresses in an infinite orthotropic sheet can be written in terms of the two stress functions ϕ_1' and ϕ_2', as follows:

$$\sigma_x(x,y) = 2Re[\mu_1^2\phi_1'(z_1) + \mu_2^2\phi_2'(z_2)] \tag{3a}$$

$$\sigma_y(x,y) = 2Re[\phi_1'(z_1) + \phi_2'(z_2)] \tag{3b}$$

$$\tau_{xy}(x,y) = -2Re[\mu_1\phi_1'(z_1) + \mu_2\phi_2'(z_2)] \tag{3c}$$

To determine the stresses for an orthotropic problem, it is necessary to formulate the stress functions $\phi_1'(z_1)$ and $\phi_2'(z_2)$ for the given loading condition and configuration.

Stress Functions

Figure 2 shows the superposition used to determine the stress functions for a pair of concentrated forces acting on a cracked, infinite orthotropic sheet. The cracked sheet with the point load applied at z_0 with the crack-face loadings needed to close the crack is shown in Fig. 2b. This loading and configuration are equivalent to an uncracked infinite sheet with a point load applied at z_0. The loading in Fig. 2b is superimposed on the crack-face loadings in Fig. 2c to produce the stress-free crack face shown in Fig. 2a.

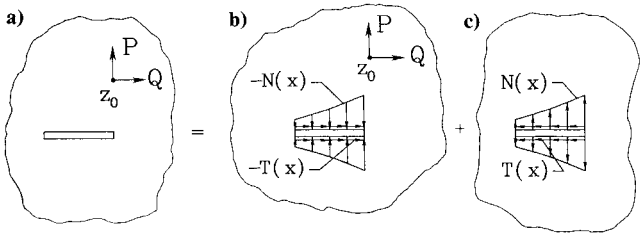

Fig. 2 Superposition of stress functions for point load in orthotropic sheet.

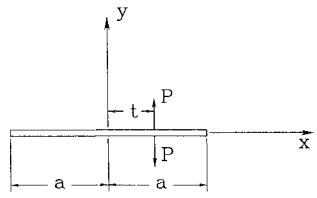

Fig. 3 Point loading on crack face.

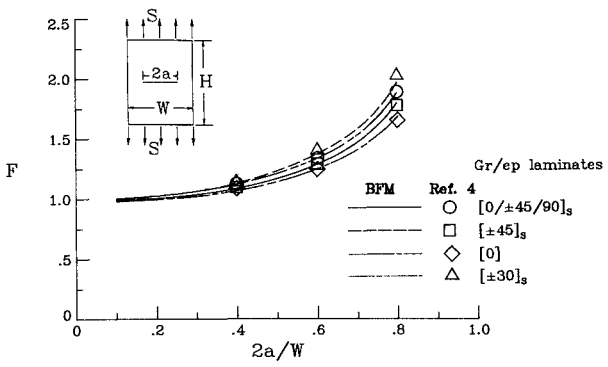

Fig. 4 Stress-intensity correction factors for a center-crack tension specimen, $H/W = 3.0$.

The stress functions for a point load in an infinite, orthotropic sheet (used for Fig. 2b) are derived from Lekhnitskii:[2]

$$\phi_1'(z_1) = [A/(z_1 - w_1)], \quad \phi_2'(z_2) = [B/(z_2 - w_2)] \tag{4}$$

where

$$A = C_{11}P + C_{12}Q, \qquad B = C_{21}P + C_{22}Q$$

$$w_j = x_0 + \mu_j y_0, \qquad z_j = x + \mu_j y, \qquad (j = 1,2)$$

$$C_{11} = \frac{\mu_1[\bar{\mu}_1(1 + \nu_{yx}\mu_2\bar{\mu}_2) + \bar{\mu}_2 + \mu_2]}{2\pi i(\mu_1 - \mu_2)(\mu_1 - \bar{\mu}_1)(\mu_1 - \bar{\mu}_2)}$$

$$C_{12} = \frac{\mu_1[(\bar{\mu}_2 + \mu_2)\bar{\mu}_1 + \mu_2\bar{\mu}_2 + \nu_{xy}]}{2\pi i(\mu_1 - \mu_2)(\mu_1 - \bar{\mu}_1)(\mu_1 - \bar{\mu}_2)}$$

$$C_{21} = \frac{\mu_2[(1 + \nu_{yx}\mu_1\bar{\mu}_1)\bar{\mu}_2 + \bar{\mu}_1 + \mu_1]}{2\pi i(\mu_2 - \mu_1)(\mu_2 - \bar{\mu}_2)(\mu_2 - \bar{\mu}_1)}$$

$$C_{22} = \frac{\mu_2[(\bar{\mu}_1 + \mu_1)\bar{\mu}_2 + \mu_1\bar{\mu}_1 + \nu_{xy}]}{2\pi i(\mu_2 - \mu_1)(\mu_2 - \bar{\mu}_2)(\mu_2 - \bar{\mu}_1)} \tag{5}$$

Here ν_{xy} and ν_{yx} are the Poisson's ratios; μ_1, μ_2, $\bar{\mu}_1$, and $\bar{\mu}_2$ are the complex roots of the characteristic equation

$$\left\{\mu^4 + \left(\frac{E_x}{G_{xy}} - 2\nu_{xy}\right)\mu^2 + \frac{E_x}{E_y} = 0\right\}$$

The barred quantities represent the complex conjugates of the underlying functions.

For isotropic materials, the roots of the characteristic equation are $\mu_1 = \mu_2 = i$. However, because of the term $(\mu_1 - \mu_2)$ in the denominator of Eqs. (5), the stress functions for orthotropic materials will not be valid for isotropic materials. In order to verify the stress functions for isotropic materials, a small perturbation was introduced in the values of μ_1 and μ_2 so that $\mu_1 = 1.0001i$ and $\mu_2 = 0.9998i$.

To find the stress functions for the loading shown in Fig. 2c, the stress functions for a point load applied at an arbitrary point on the crack face are used. From Savin[3] the stress functions for this loading are

$$\phi_1'(z_1) = \frac{-\mu_2 P - Q}{2\pi(\mu_1 - \mu_2)} \frac{1}{\sqrt{z_1^2 - a^2}} \frac{\sqrt{a^2 - t^2}}{z_1 - t} \tag{6a}$$

$$\phi_2'(z_2) = \frac{-\mu_1 P + Q}{2\pi(\mu_1 - \mu_2)} \frac{1}{\sqrt{z_2^2 - a^2}} \frac{\sqrt{a^2 - t^2}}{z_2 - t} \tag{6b}$$

where P and Q are the normal and tangential point loads applied to the crack face, and t is the location of the load point on the crack face $(-a < t < a)$ as shown in Fig. 3.

By integrating Eqs. (6) over the crack face, the stress functions for the nonuniform distributed loads applied to the crack face can be written as

$$\phi_1'(z_1) = \frac{-1}{2\pi(\mu_1 - \mu_2)} \frac{1}{\sqrt{z_1^2 - a^2}} \int_{-a}^{a} [\mu_2 N(\xi) + T(\xi)] \frac{\sqrt{a^2 - \xi^2}}{z_1 - \xi} d\xi \tag{7a}$$

$$\phi_2'(z_2) = \frac{1}{2\pi(\mu_1 - \mu_2)} \frac{1}{\sqrt{z_2^2 - a^2}} \int_{-a}^{a} [\mu_1 N(\xi) + T(\xi)] \frac{\sqrt{a^2 - \xi^2}}{z_2 - \xi} d\xi \tag{7b}$$

In order to erase the stresses along the crack line $-a < x < a$, the loadings $N(x)$ and $T(x)$ are specified to be the same as the stresses found in the equivalent uncracked sheet shown in Fig. 2b. That is, $N(x) = \sigma_y(x,0)$ and $T(x) = \tau_{xy}(x,0)$. Thus, from Eqs. (3) and (4), the normal and shear stresses on the line $y = 0$ are

$$\sigma_y(x,0) = 2Re\left(\frac{A}{x - w_1} + \frac{B}{x - w_2}\right) \tag{8a}$$

$$\tau_{xy}(x,0) = -2Re\left(\frac{\mu_1 A}{x - w_1} + \frac{\mu_2 B}{x - w_2}\right) \tag{8b}$$

Using Eqs. (8) and remembering that $2Re[f(z)] = f(z) + \overline{f(z)}$, the loading functions in the integrands in Eqs. (7) can be simplified as

$$\mu_2 N(x) + T(x) = 2\mu_2 Re\left(\frac{A}{x - w_1} + \frac{B}{x - w_2}\right) - 2Re\left(\frac{\mu_1 A}{x - w_1} + \frac{\mu_2 B}{x - w_2}\right) = \frac{(\mu_2 - \mu_1)A}{x - w_1} + \frac{(\mu_2 - \bar{\mu}_1)\bar{A}}{x - \bar{w}_1} + \frac{(\mu_2 - \bar{\mu}_2)\bar{B}}{x - \bar{w}_2} \tag{9a}$$

$$\mu_1 N(x) + T(x) = 2\mu_1 Re\left(\frac{A}{x - w_1} + \frac{B}{x - w_2}\right) - 2Re\left(\frac{\mu_1 A}{x - w_1} + \frac{\mu_2 B}{x - w_2}\right) = \frac{(\mu_1 - \mu_2)B}{x - w_2} + \frac{(\mu_1 - \bar{\mu}_1)\bar{A}}{x - \bar{w}_1} + \frac{(\mu_1 - \bar{\mu}_2)\bar{B}}{x - \bar{w}_2} \tag{9b}$$

Substituting these expressions into Eqs. (7), integrating, and then adding Eqs. (4), the following expressions are found for

the stress functions for the loading shown in Fig. 2a:

$$\phi_1'(z_1) = \frac{1}{2(\mu_1 - \mu_2)\sqrt{z_1^2 - a^2}}\left[\frac{(\mu_2 - \mu_1)A}{z_1 - w_1} f(z_1, w_1, a) + \frac{(\mu_2 - \bar{\mu}_1)\bar{A}}{z_1 - \bar{w}_1} f(z_1, \bar{w}_1, a) + \frac{(\mu_2 - \bar{\mu}_2)\bar{B}}{z_1 - \bar{w}_2} f(z_1, \bar{w}_2, a)\right] + \frac{A}{z_1 - w_1} \quad (10a)$$

$$\phi_2'(z_2) = \frac{-1}{2(\mu_1 - \mu_2)\sqrt{z_2^2 - a^2}}\left[\frac{(\mu_1 - \mu_2)B}{z_2 - w_2} f(z_2, w_2, a) + \frac{(\mu_1 - \bar{\mu}_1)\bar{A}}{z_2 - \bar{w}_1} f(z_2, \bar{w}_1, a) + \frac{(\mu_1 - \bar{\mu}_2)\bar{B}}{z_2 - \bar{w}_2} f(z_2, \bar{w}_2, a)\right] + \frac{B}{z_2 - w_2} \quad (10b)$$

where $f(z, w, a) = \sqrt{z^2 - a^2} - \sqrt{w^2 - a^2} - z + w$. (These stress functions are identical to those presented by Snyder and Cruse,[4] derived by formulating the problem as a Hilbert problem.)

Once the stress functions are known, it is a simple step to calculate the stresses at any point in the body using Eqs. (3). Then, as explained earlier, the stresses are integrated over each segment length to obtain resultant forces for use in Eq. (2).

Stress-Intensity Factor Equation

From Sih and Liebowitz,[5] the mode *I* stress-intensity factor for orthotropic materials may be expressed in terms of the stress functions as

$$K_I = 2\sqrt{2\pi}\,\frac{\mu_2 - \mu_1}{\mu_2} \lim_{z_1 \to a} \{\sqrt{z_1 - a}\,[\phi_1'(z_1)]\}$$

By substituting from Eq. (10) into the above equation and taking the limit, the mode *I* stress-intensity factor for a point load in an infinite cracked orthotropic sheet may be written as

$$K_I = \frac{1}{\mu_2\sqrt{a}}\left[(\mu_2 - \mu_1)A\, g(w_1, a) + (\mu_2 - \bar{\mu}_1)\bar{A}\, g(\bar{w}_1, a) + (\mu_2 - \bar{\mu}_2)\bar{B}\, g(\bar{w}_2, a)\right]$$

where

$$g(w, a) = \frac{\sqrt{w - a}\,\sqrt{w + a} - w + a}{w - a}$$

Results and Discussion

Four graphite/epoxy (gr/ep) laminates, covering a wide range of properties, were used in the analysis; these laminates were the quasi-isotropic layup $[0/\pm 45/90]_s$, $[0]$, $[\pm 45]_s$, and $[\pm 30]_s$. Table 1 presents the laminate constants for the four laminates. The 0 deg lamina properties[4] were used with lamination theory to calculate the elastic constants for the other laminates. (Here, the 0 deg direction is defined parallel to the load axis.) Although the $[0/\pm 45/90]_s$ laminate is called a quasi-isotropic laminate, its calculated elastic constants satisfy all the criteria for isotropy. Consequently, the results for this laminate were compared with isotropic solutions from the literature. To show the effects of the specimen boundaries, the results are presented using the stress-intensity correction factor *F* from

$$K_I = S\sqrt{\pi a}\, F$$

Table 1 Laminate constants

Laminate	E_x, GPa	E_y, GPa	ν_{xy}	G_{xy}, GPa
$[0/\pm 45/90]_s$	60.04	60.04	0.259	23.85
$[0]$	11.72	144.8	0.017	9.65
$[\pm 45]_s$	31.18	31.18	0.615	38.03
$[\pm 30]_s$	17.64	66.99	0.262	30.94

Verification of Analysis

To evaluate the BFM for orthotropic materials, the BFM stress-intensity factor solutions are compared to results from the literature for a center-crack plate subjected to uniaxial tension.

A convergence study was done using the center-crack tension specimen. The number of degrees of freedom (DOF) was varied from 20 to 124 for each of the laminates given in Table 1. The layup had no effect on the convergence rate; all solutions converged with fewer than 100 DOF. (Increasing the number of DOF from 64 to 124 changed the value of *F* less than 0.14%.) Thus, a boundary mesh with approximately 100 DOF was used for the remainder of the analyses. The radial-line method[1] was used to generate the mesh points. This method produces smaller line segments on the boundaries near the crack tip and larger line segments on the boundaries away from the crack tip. With the radial-line method of modeling, it is possible to model the same problem with fewer DOF, compared to a mesh with equal-size segments, without sacrificing accuracy.[1] An offset δ_i of one-quarter of the segment length was used to eliminate the singularities in the stress calculations.

As mentioned earlier, the present formulation of the BFM uses only forces to approximate the given boundary conditions, whereas the BFM formulated by Tan et al.[1] uses both forces and moments. The absence of moments requires a greater number of DOF to achieve the same accuracy compared to a solution including moments. The absence of the moments is believed to have no effect on the accuracy of the solution, but more DOF are required to achieve the same accuracy.

The BFM results for the quasi-isotropic laminate for the center-crack specimen with $H/W = 3.0$ were compared to an accepted collocation solution for the same configuration in an isotropic material.[6] The two solutions agreed within 0.005%.

Figure 4 compares the present BFM results with results from Snyder and Cruse[4] for a center-crack tension specimen with $H/W = 3.0$. The curves represent the BFM calculations, and the symbols indicate the values taken from Snyder and Cruse. The stress-intensity correction factors calculated by the BFM agree, within ± 3%, with the values from Snyder and Cruse for all laminates considered. For the $[0/\pm 45/90]_s$ laminate at $2a/W = 0.8$, the solution from Snyder and Cruse was 2% lower than the solution for an isotropic material,[6] whereas the BFM solution for the $[0/\pm 45/90]_s$ laminate was only in error by 0.005% compared to the accepted isotropic solution. Therefore, for the other laminates considered, the 3% difference between the present results and those of Snyder and Cruse is acceptable.

For small crack lengths, the stress-intensity factor was not influenced by specimen width; *F* was near unity for all layups. For longer cracks, the finite width of the laminate elevated *F*. The boundary effect was different for different layups. The results from both the BFM and Snyder and Cruse[4] showed that the *F* values for the laminates containing angle plies are higher than for the quasi-isotropic laminate. The *F* values found for the [0] laminate are below the quasi-isotropic results.

Hole Solutions

Two other cases for which orthotropic solutions currently are not available were analyzed. Stress-intensity correction factors for cracks emanating from a circular hole are presented for a range of crack length-to-width ratios. This configuration is used to examine the effects of a hole on stress-intensity factors. Also analyzed was a four-hole specimen with a center crack[1] used to simulate a stringer. Because of symmetry, only one-quarter of the specimen was modeled in each configuration.

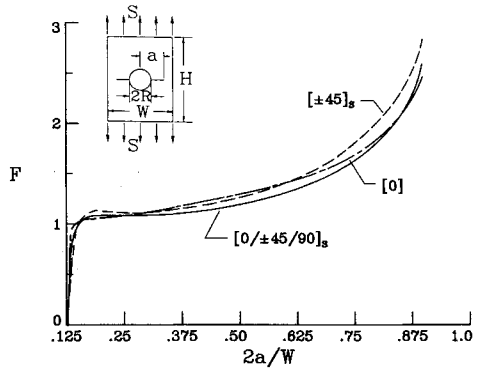

Fig. 5 Stress-intensity correction factors for edge cracks emanating from a circular hole, $2R/W = 0.125$, $H/W = 2.0$.

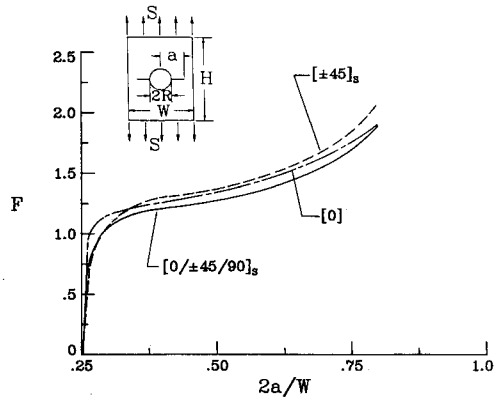

Fig. 6 Stress-intensity correction factors for edge cracks emanating from a circular hole, $2R/W = 0.25$, $H/W = 2.0$.

Cracks from a Circular Hole

Figures 5 through 7 and Tables 2, 3, and 4 show the stress-intensity correction factors for two cracks emanating from a circular hole using three values of the hole radius-to-width ratio ($2R/W = 0.125$, 0.25, and 0.50). Three graphite/epoxy laminates were used in this configuration: $[0/\pm 45/90]_s$, [0], and $[\pm 45]_s$. For all $2R/W$ ratios considered, the [0] laminate showed a steeper initial slope compared to the other laminates. That is, for very small values of $2a/W$, when the effect of the hole was dominant, the [0] laminate gave the highest value of F. This agrees with the calculations of Lekhnitskii[2] for circular holes in infinite orthotropic sheets, where his analysis calculated higher stress concentrations for a [0] laminate compared to a quasi-isotropic laminate. As $2a/W$ increased, the F values for both the [0] and the $[\pm 45]_s$ laminates were greater than for the quasi-isotropic case, where the $[\pm 45]_s$ laminate had the largest values of F. Then, as the crack approached the edge of the laminate ($2a/W > 0.6$), where the effect of the hole is negligible, the [0] laminate gave the lowest values of F. This agrees with the results for the center-crack specimen previously shown in Fig. 4, where the [0] laminate gave the lowest values of F, and the $[\pm 45]_s$ laminate gave the highest values of F.

Four-Hole Crack Specimen

Stringers are widely used in aircraft structures as stiffening members. The four-hole crack specimen shown in Fig. 8 simulates the effect of stringers on the stress-intensity factor.

The stress-intensity correction factors obtained for a range of crack length-to-width ratios ($0 < a/w < 0.9$) are presented in Fig. 8 and Table 5. Results are plotted for four graphite/epoxy laminates: $[0/\pm 45/90]_s$, [0], $[\pm 45]_s$, and $[\pm 30]_s$. For comparison, Fig. 8 also shows the curves for the cracked laminates

Table 2 Stress-intensity correction factors for edge cracks emanating from a circular hole, $2R/W = 0.125$, $H/W = 2.0$

	F for graphite/epoxy laminates		
$2a/W$	$[0/\pm 45/90]_s$	$[\pm 45]_s$	[0]
0.125	0.0	0.0	0.0
0.13	0.6185	0.5383	0.8615
0.14	0.9005	0.8513	1.0158
0.16	1.0524	1.0834	1.0557
0.20	1.0911	1.1330	1.0679
0.24	1.0907	1.1209	1.0841
0.28	1.0935	1.1186	1.1064
0.36	1.1174	1.1594	1.1658
0.50	1.2105	1.2791	1.3011
0.60	1.3263	1.4242	1.4225
0.70	1.5110	1.6413	1.5854
0.80	1.8401	2.0314	1.8487
0.90	2.6045	2.8448	2.4761

Table 3 Stress-intensity correction factors for edge cracks emanating from a circular hole, $2R/W = 0.25$, $H/W = 2.0$

	F for graphite/epoxy laminates		
$2a/W$	$[0/\pm 45/90]_s$	$[\pm 45]_s$	[0]
0.25	0.0	0.0	0.0
0.26	0.6577	0.5829	0.9407
0.28	0.9600	0.9260	1.1179
0.30	1.0767	1.1009	1.1628
0.40	1.2145	1.3109	1.2538
0.50	1.2842	1.3706	1.3542
0.60	1.3955	1.4954	1.4793
0.70	1.5796	1.7020	1.6432
0.80	1.9063	2.0677	1.9054

Table 4 Stress-intensity correction factors for edge cracks emanating from a circular hole, $2R/W = 0.50$, $H/W = 2.0$

	F for graphite/epoxy laminates		
$2a/W$	$[0/\pm 45/90]_s$	$[\pm 45]_s$	[0]
0.5	0.0	0.0	0.0
0.52	0.8804	0.8279	1.2739
0.53	1.0308	0.9947	1.3877
0.54	1.1420	1.1254	1.4589
0.55	1.2296	1.2346	1.5090
0.60	1.5018	1.6127	1.6551
0.70	1.8241	2.0358	1.8680
0.80	2.1980	2.4085	2.1488
0.90	2.9467	3.1241	2.7460

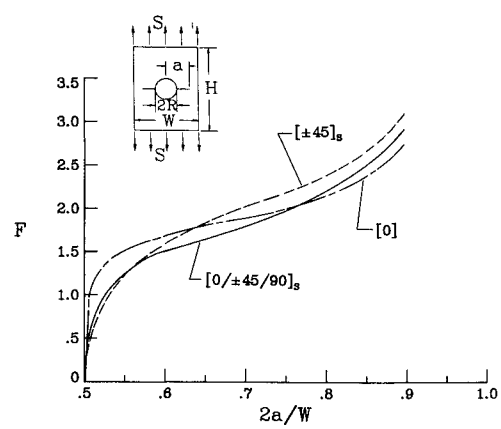

Fig. 7 Stress-intensity correction factors for edge cracks emanating from a circular hole, $2R/W = 0.5$, $H/W = 2.0$.

Table 5 Stress-intensity correction factors for four-hole cracked specimen

	F for graphite/epoxy laminates			
a/W	$[0/\pm 45/90]_s$	$[\pm 45]_s$	[0]	$[\pm 30]_s$
0.05	1.1756	1.2244	1.0728	1.1657
0.10	1.1914	1.2505	1.1048	1.1797
0.15	1.2216	1.3025	1.1230	1.2151
0.20	1.2674	1.3671	1.1694	1.2720
0.25	1.3305	1.4301	1.2235	1.3587
0.30	1.4124	1.4785	1.3377	1.4698
0.35	1.4795	1.4937	1.5560	1.5679
0.375	1.4961	1.4694	1.6763	1.5901
0.40	1.4881	1.4420	1.7389	1.5796
0.425	1.4444	1.4091	1.6097	1.5268
0.45	1.3599	1.3732	1.3117	1.4180
0.475	1.2404	1.3437	1.0527	1.2567
0.50	1.1063	1.3077	0.8404	1.0653
0.525	0.9886	1.2599	0.6231	0.8964
0.55	0.9163	1.1952	0.4279	0.7979
0.575	0.9036	1.1368	0.4405	0.7910
0.60	0.9462	1.1136	0.6792	0.8622
0.65	1.1259	1.1814	1.1626	1.1307
0.70	1.3420	1.3861	1.3843	1.4180
0.75	1.5565	1.6411	1.5513	1.6615
0.80	1.7951	1.9455	1.7476	1.9080
0.85	2.1058	2.3130	1.9975	2.2226
0.90	2.6028	2.8339	2.3880	2.7291

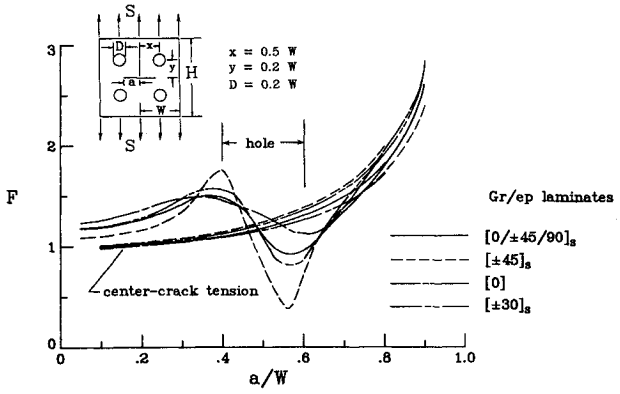

Fig. 8 Stress-intensity correction factors for a four-hole specimen, $H/W = 3.0$.

without the holes (shown previously in Fig. 4). The results for the four-hole specimen show that the stress-intensity correction factors increased (above the results for the center-crack specimen) as the crack tip approached the inner edge of the hole. However, as the crack tip approached the centerline of the holes, the stress-intensity correction factors decreased (below the results for the center-crack specimen) until a minimum value was reached. This drop in the stress-intensity correction factors is due to the shielding of the crack tip by the holes from the externally applied stress field. This is similar to the behavior seen for the same configuration in an isotropic material.[1] The results shown here for the quasi-isotropic laminate were in excellent agreement with the isotropic results.

As the crack tip approached the holes, the values for the [0] laminate rose to a sharp peak above the quasi-isotropic values and then, as the crack tip approached the centerline of the holes, the values for the [0] laminate dropped well below the quasi-isotropic values. Finally, as the crack passed the holes, the values for the [0] laminate increased more rapidly than the other laminates at first and then again dropped below the quasi-isotropic values. The two angle ply laminates showed similar, but not as dramatic, behavior with the $[\pm 45]_s$ laminate showing the smallest drop due to the presence of the hole.

Concluding Remarks

In this paper, the Boundary Force Method (BFM), a form of an indirect boundary element method, was used to analyze composite laminates with holes and cracks. The BFM uses the elasticity solution for a concentrated horizontal and vertical force applied at a point in a cracked, infinite orthotropic sheet as the fundamental solution. The necessary stress functions for this fundamental solution were formulated using the complex variable theory of orthotropic elasticity. The orthotropic formulation of the BFM was verified by comparison to accepted solutions for a center-crack specimen subjected to uniaxial tension with a variety of material properties. The BFM results agreed well with accepted solutions. For the center-crack specimen, the boundary effects were different for different materials. The [0] laminate gave the lowest stress-intensity correction factors, whereas $[\pm 45]_s$ laminate gave the highest values.

Two configurations for which no orthotropic solutions are currently available were analyzed. Parametric studies were done for cracks emanating from a circular hole and for a four-hole cracked specimen, both loaded in uniaxial tension with a variety of materials properties.

In the specimen with cracks emanating from a hole, for small $2a/W$ ratios, when the hole dominated, the [0] laminate gave the highest stress-intensity correction factors, and the $[\pm 45]_s$ laminate gave the lowest values. For larger $2a/W$, when the effect of the hole had diminished, the trends were reversed, and the [0] laminate gave the lowest values of the stress-intensity correction factor; the $[\pm 45]_s$ laminate gave the highest values, corresponding to the trend seen in the center-crack tension specimen.

For the four-hole specimen, in all laminates considered, the stress-intensity correction factors increased as the crack tip approached the hole, dropped as the crack tip approached the centerline of the holes, and then increased again as the crack tip passed the holes. The [0] laminate was the most sensitive to the presence of the holes, showing the greatest rise and drop in the stress-intensity correction factor as the crack approached and passed the hole. The stress-intensity correction factors for the $[\pm 45]_s$ laminate showed the least effect due to the hole.

Although the present formulation of the BFM uses only forces to approximate the given boundary conditions, the absence of the moments had no effect on the accuracy of the solution. Convergence was slower when the moments are not included; thus, more boundary elements were required to achieve the same accuracy.

This work has resulted in the extension of the BFM to the analysis of composite laminates with cracks and notches. This method yields accurate solutions with minimal modeling effort, even for complex configurations. The accurate stress-intensity factors obtained with this method should be useful in predicting fracture strengths of arbitrarily shaped composite laminates.

References

[1]Tan, P. W., Raju, I. S., and Newman, J. C. Jr., "Boundary Force Method for Analyzing Two-Dimensional Cracked Bodies," NASA TM-87725, May 1986.

[2]Lekhnitskii, S. G., *Anisotropic Plates,* translated by S. W. Tsai and T. Cheron, Gordon & Breach, New York, 1968.

[3]Savin, G. N., "Stress Distribution Around Holes," NASA Technical Translation F-607, Nov. 1970.

[4]Snyder, M. D. and Cruse, T. A., "Crack Tip Stress Intensity Factors in Finite Anisotropic Plates," Air Force Materials Lab., Wright-Patterson AFB, OH, AFML-TR-73-209, Aug. 1973.

[5]Sih, G. C. and Liebowitz, H., "Mathematical Theories of Brittle Fracture," *Fracture—An Advanced Treatise: Volume II—Mathematical Fundamentals,* H. Liebowitz, ed., Academic, New York, 1968, pp. 67–190.

[6]Newman, J. C. Jr., "An Improved Method of Collocation for the Stress Analysis of Cracked Plates with Various Shaped Boundaries," NASA TN D-6376, Aug. 1971.